eHeroes 

Evolutionary pattern of DEM variations in flare(s)

B. Sylwester, J. Sylwester, A. Kępa, T. Mrozek
Space Research Centre, PAS, Wrocław, Poland
K.J.H. Phillips
Natural History Museum, London, UK
V.D. Kuznetsov
IZMIRAN, Moscow, Russia

ApJ submitted, is after the first iteration with the Referee

Average RESIK spectrum spectrum (integrated over 26.5 min) for M1.0 flare

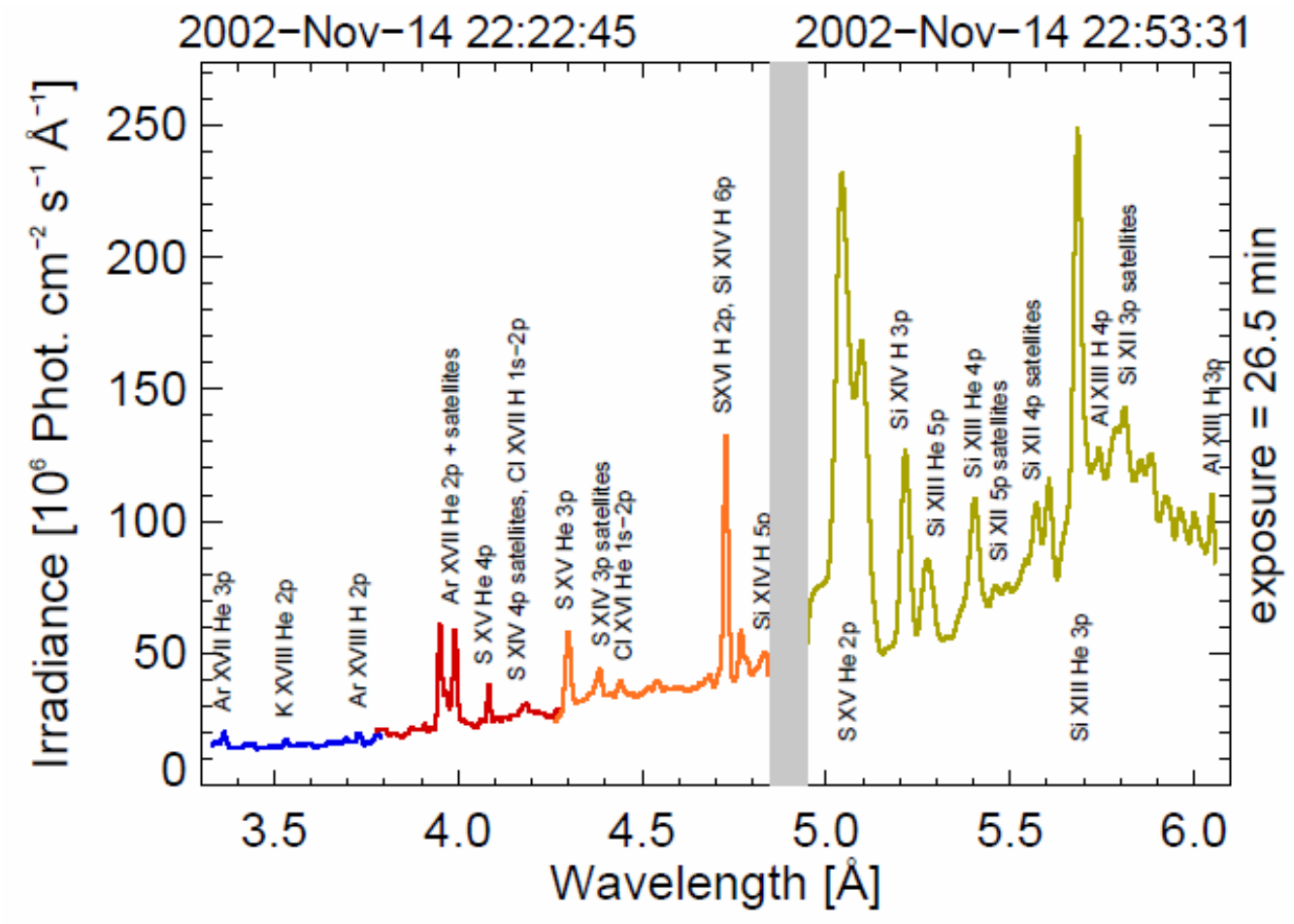

Well observed flare, 127 individual spectra available,
that we summed over 19 time intervals for detailed analysis.

SOL2002-11-14T22:26
normalised lightcurves

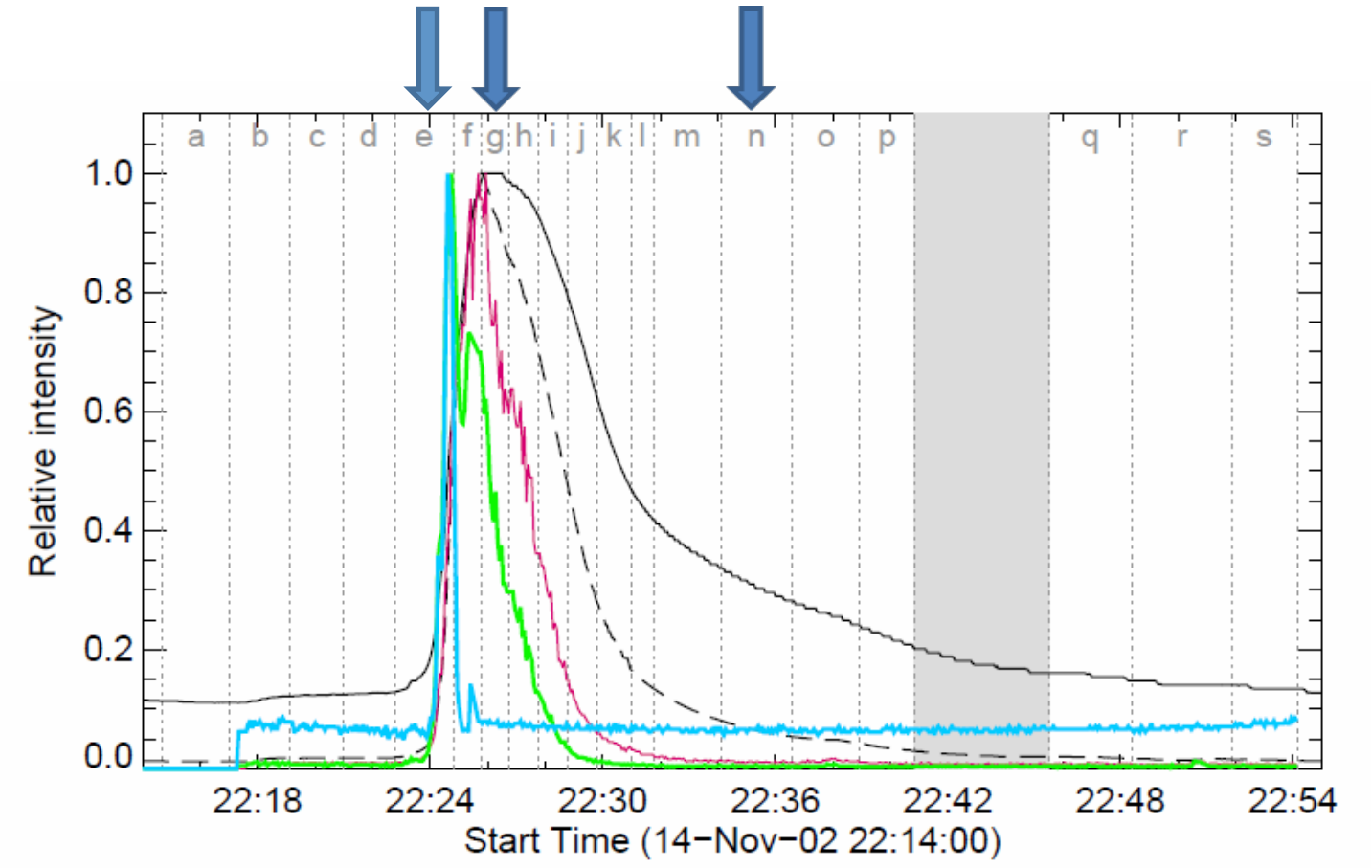

GOES

0.5 – 4 Å ----

1 – 8 Å ——

RHESSI

6 – 12 keV

12 – 25 keV

25 – 50 keV

19 time intervals selected (a-s) → Sample spectra for: rise (**e**), maximum (**g**) and decay (**n**) phases

Spectra evolution: SOL2002-11-14T22:26

different colours-individual spectral channels

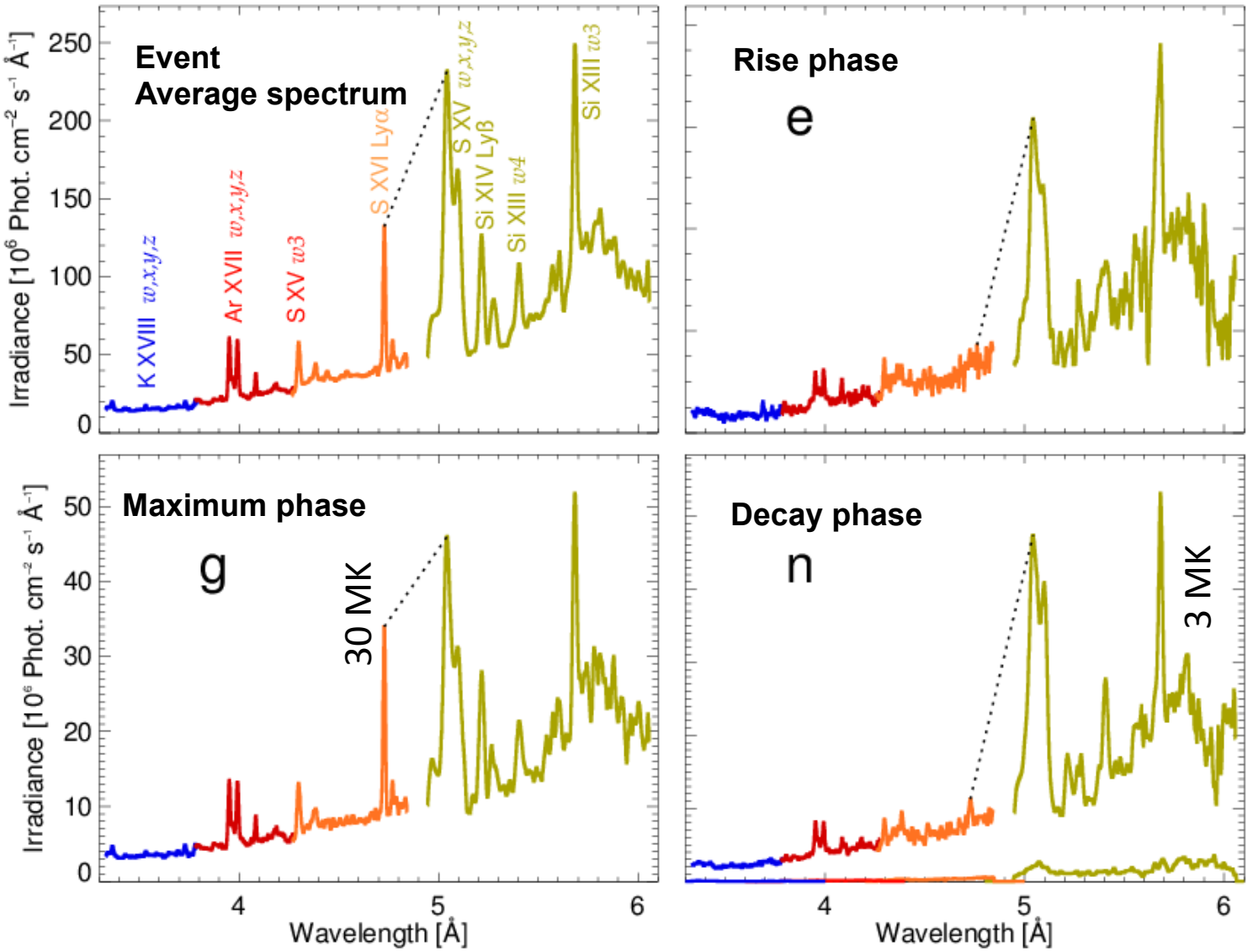

RESIK - Bragg bent crystal spectrometer: NRL, MSSL, RAL, IZMIRAN

4 x

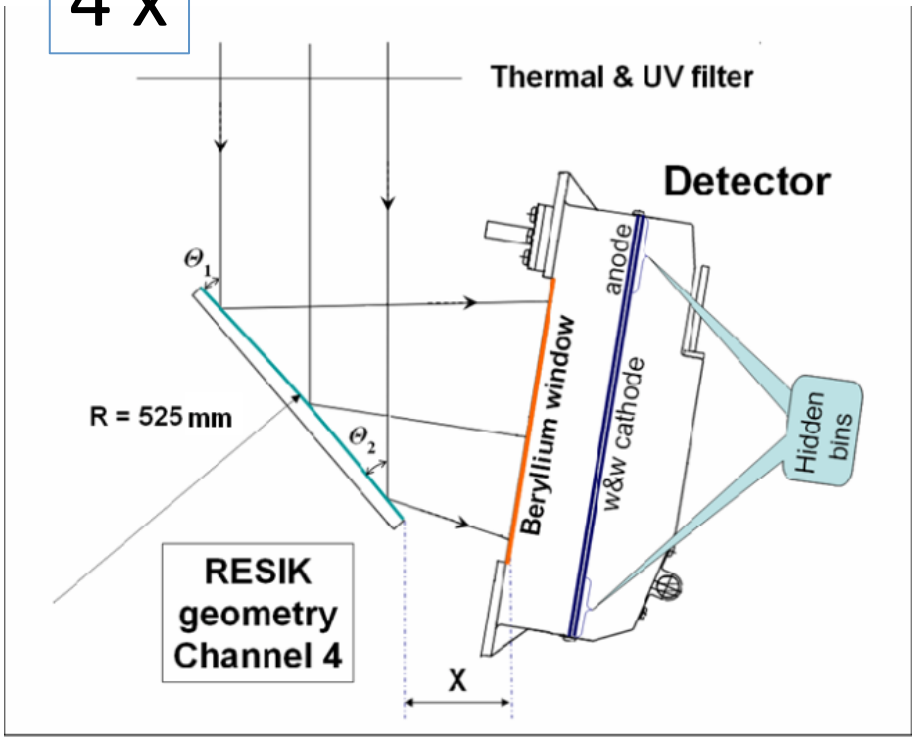

RESIK aboard the Russian ***CORONAS-F*** satellite.

It observed solar coronal spectra in four energy bands over **~3.3 Å – 6.1 Å** band (~800 spectral bins)

Operational in 2002 and first part of 2003

~ 2 mln spectra available, 6000 reduced to Level2 (60 flares). Data in the public domain http://www.cbk.pan.wroc.pl/experiments/resik/RESIK_Level2/index.html

Selection of spectral bands (for inversion)

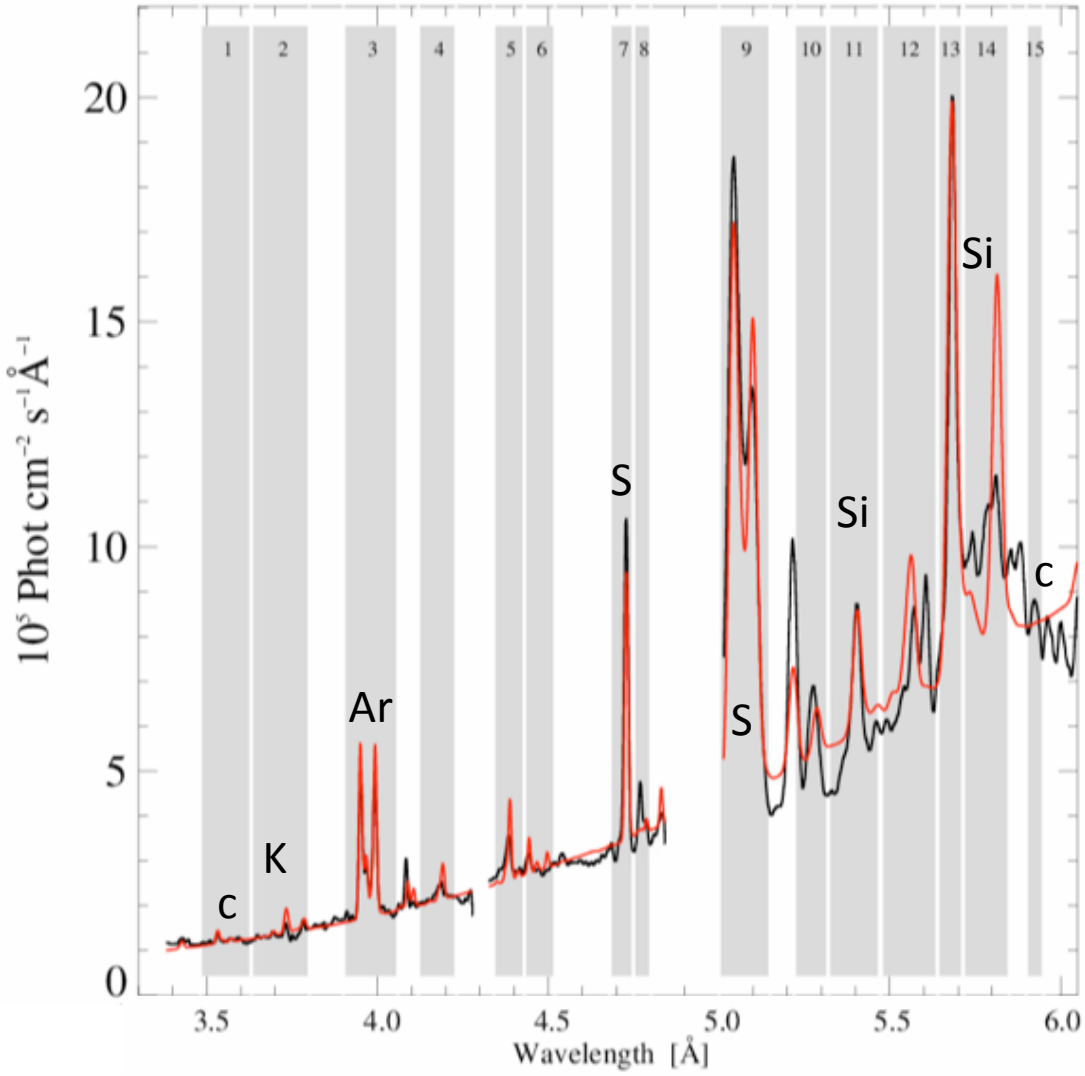

15 bands:

- Most of them contain prominent lines of abundant elements
  K, Ar, S & Si + cont.

- Some preferentially the continuum

For every selected time (interval: a, b..) we take from observations the set of 15 fluxes F_i

The inversion:
15 measured fluxes for optically thin plasma

$$F_i = A_i \int_{T=0}^{\infty} f_i(T)\varphi(T)\mathrm{d}T$$

?

$$DEM \equiv \varphi(T) \equiv N_e{}^2 \frac{\mathrm{d}V}{\mathrm{d}T}$$

DEM → always positive, characterizes how much of plasma is present at a particular temperature interval dT (notwithstanding where within FOV)

$f_i(T)$ → CHIANTI (7.0) emission (contribution) function for each predefined spectral band,

Tables of $A_i * f_i(T)$ have been calculated for a grid of A_{EL} & T (days of calculation using CHIANTI)

Just to show how important is “pre-assumption” of composition on the inversion

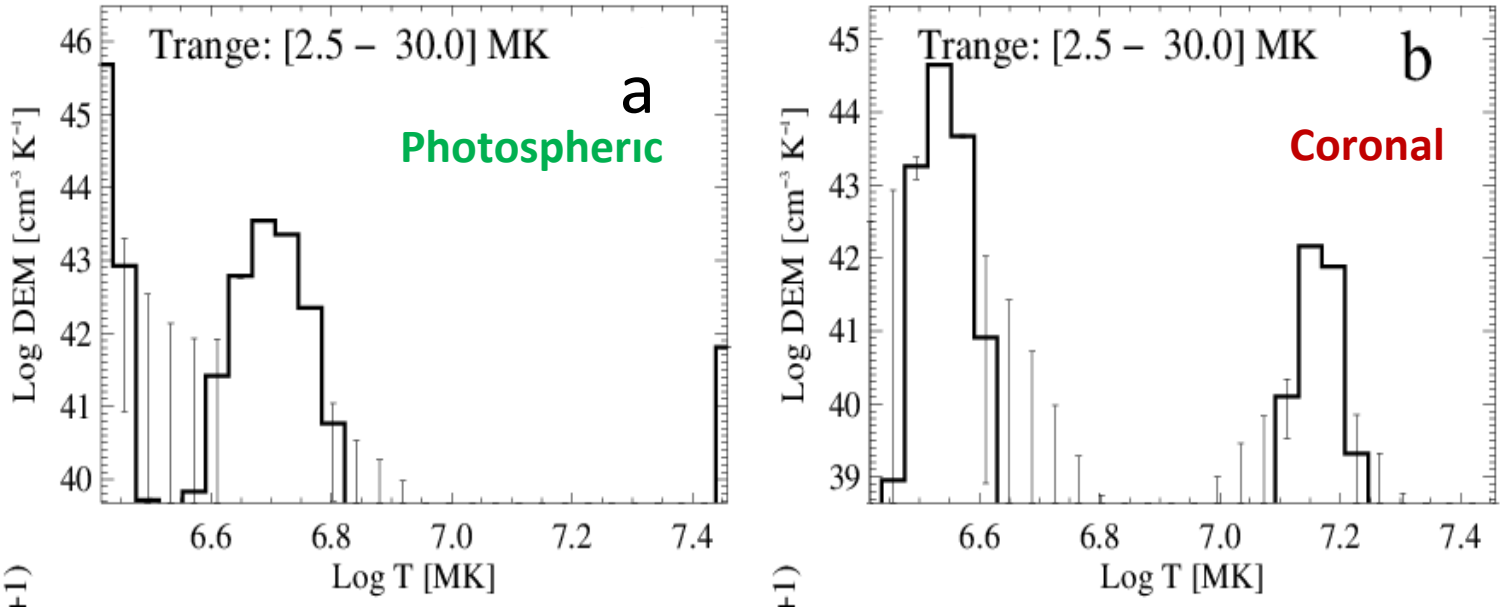

Identical sets of input fluxes have been used for a and b.
The Withbroe-Sylwester iterative algorithm corresponding to the maximum likelihood Bayesian procedure (Solar Phys., 67, 1980,) has been used for invertion.
The **kernel fluxes** have been calculated based on the CHIANTI 7.0 code with adopted **Photospheric** and **Coronal** plasma composition respectively.
Bryans ionization equilibrium has been adopted (ApJ, 691, 2009). 10 000 iterations have been performed in the accelerated scenario and the errors have been estimated from 100 Monte Carlo realizations of DEM calculations.

Dramatically different distribution of plasma DEM are unveiled for these different abundance sets

The „AbuOpt" approach

- The **emission functions** for inversion were generated for a number of following abundance pattern scenarios:
- For every important element : K, Ar, S & SI the values of kernel $A_i * f_i(T)$ were calculated for a set of abundances ranging from
  0.1 to 16 times the accepted „coronal" value of abundance
  i.e. **21 different values of abundances for particular element**
- While changing the abundance of an element „in question", the other elements' abundances were being kept to their coronal values when generating the kernel functions.
- We „tried" to fit (make inversion) of the observed fluxes for all calculated abundance patterns (~80) using the multitemperature approach (WS)
- We ALWAYS stopped the calculations at the iteration step 1000 and looked for the quality of the fit as expressed in terms of χ^2

AbuOpt results (S, Si) „flare averaged”

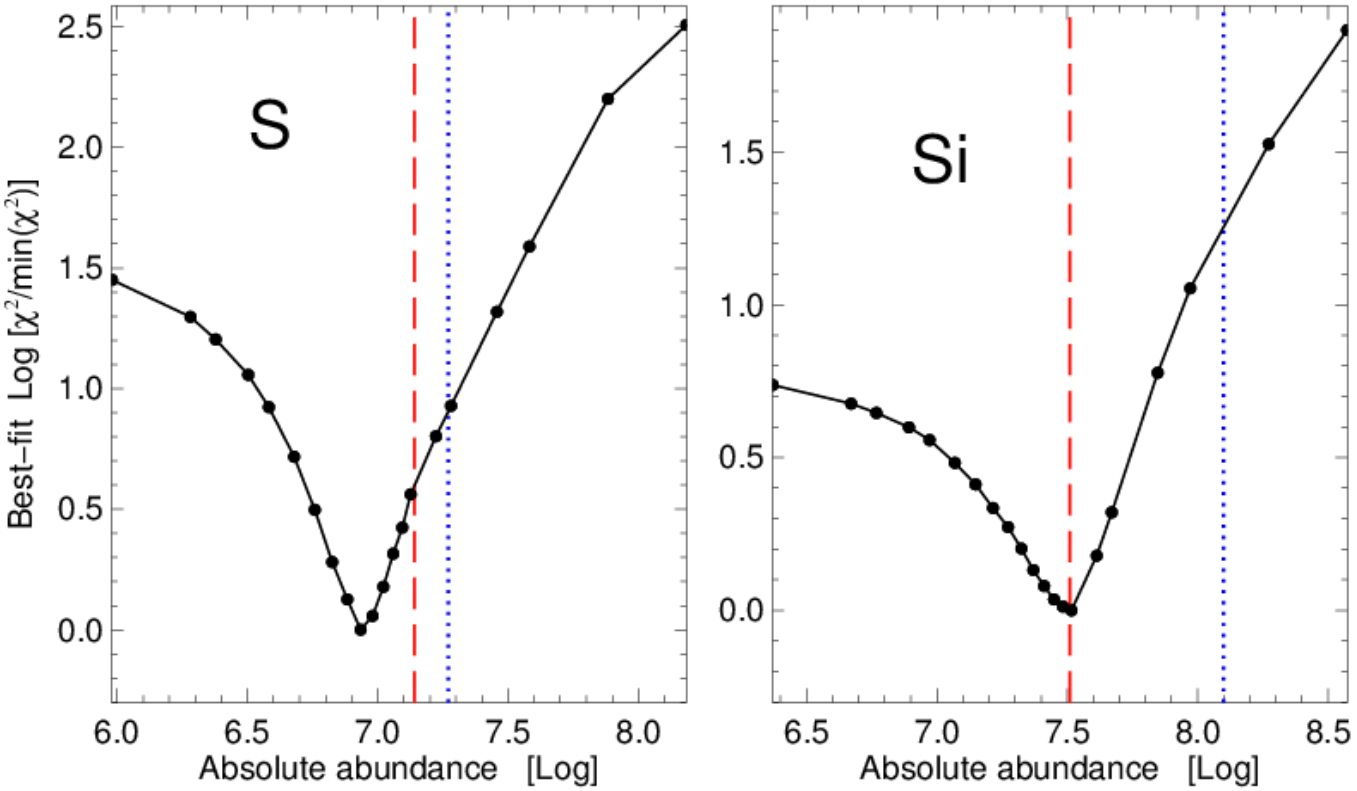

We interpret the results of the exercise that the abundance corresponding to the minimum χ^2 is the optimum one for an element in question.
Dashed red line denotes the photospheric and dotted blue the coronal abundances respectively.
We repeated the exercise for all 19 selected individual time intervals covering all phases of the flare.

AbuOpt results for individual time intervals

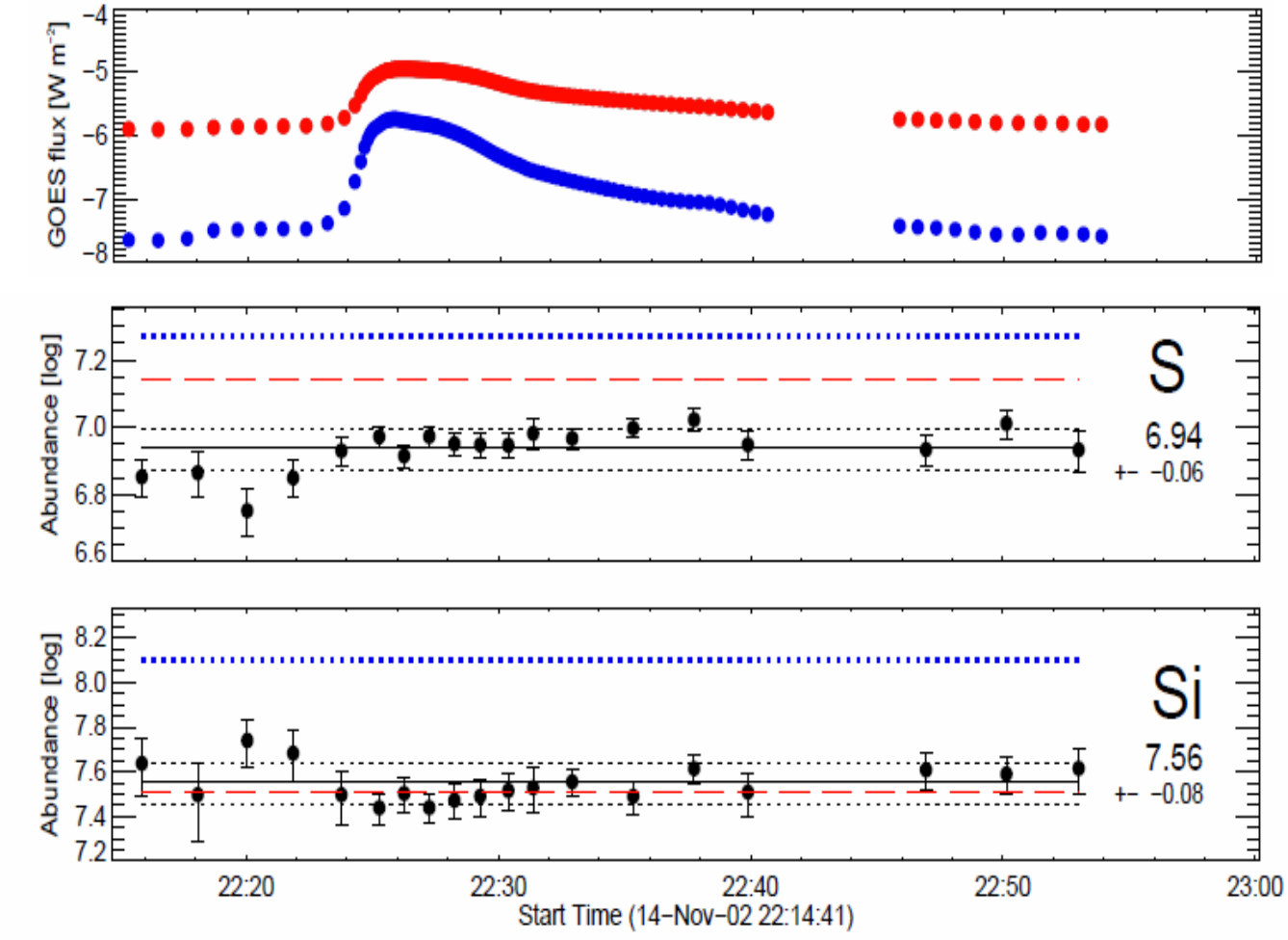

By adopting these new, flare averaged abundances we may proceed to calculate „real” DEM distributions for individual time intervals using the WS iterative procedure. Calculations have been carried out over the temperature range 2 - 30 MK. Going up to 10 000 iterations.

Variations of DEM distributions

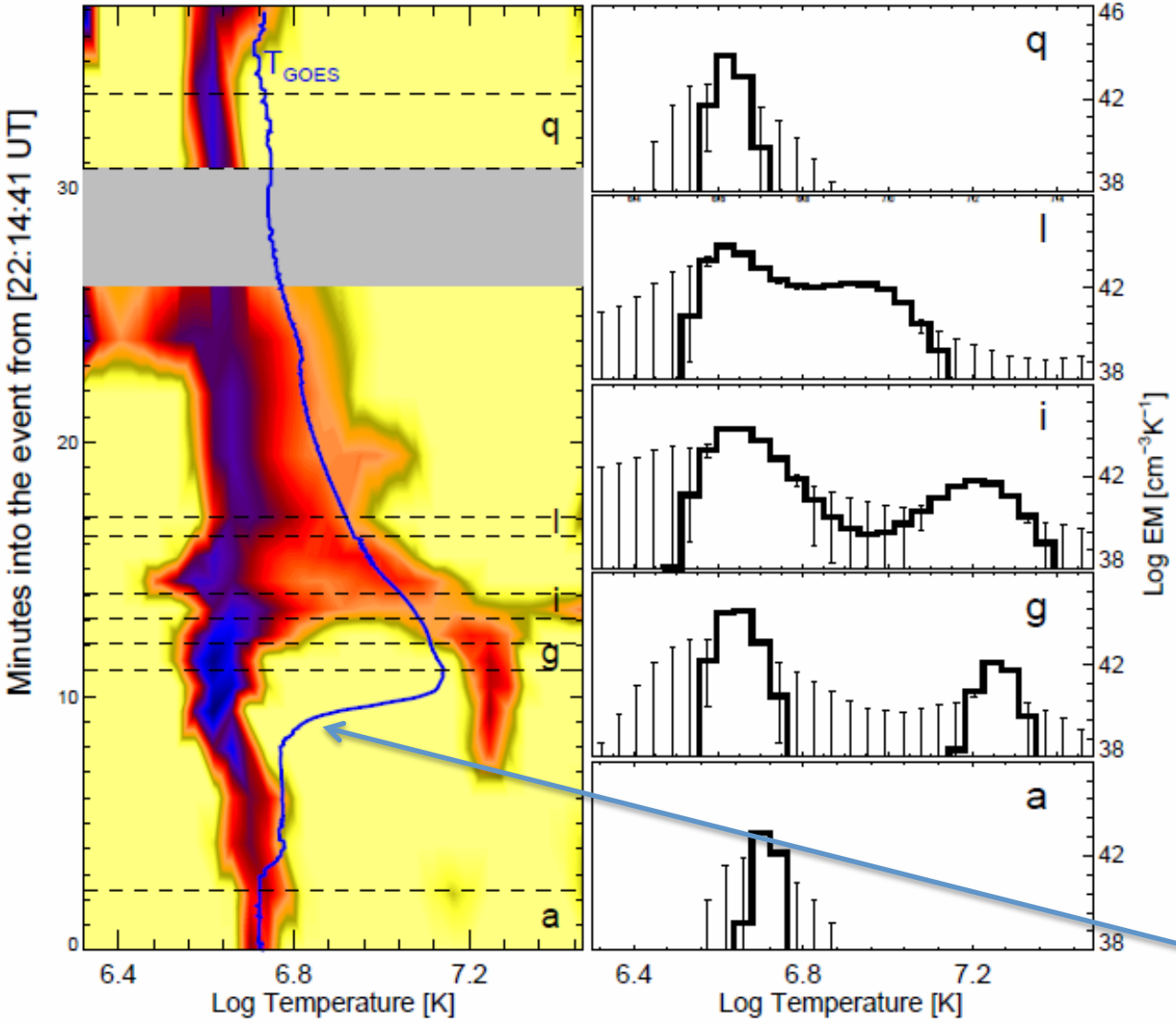

Right: Emission measure distributions for the intervals indicated in the left plot, derived using the WS routine. Vertical error bars indicate uncertainties. A cooler component (**3 - 6 MK**) is present all over the flare, and the hotter (**~16 - 21 MK**) component is visible during the main rise and max phases. with the EM ~100 times smaller.

Left: DEM during SOL2002-11-14T22:26 flare, blue shades show larger EM (log scaling) . Horizontal dotted lines define the time intervals a, g, i, l, and q.

The *GOES* temperature course is overplotted

RHESSI images: the hotter source extension

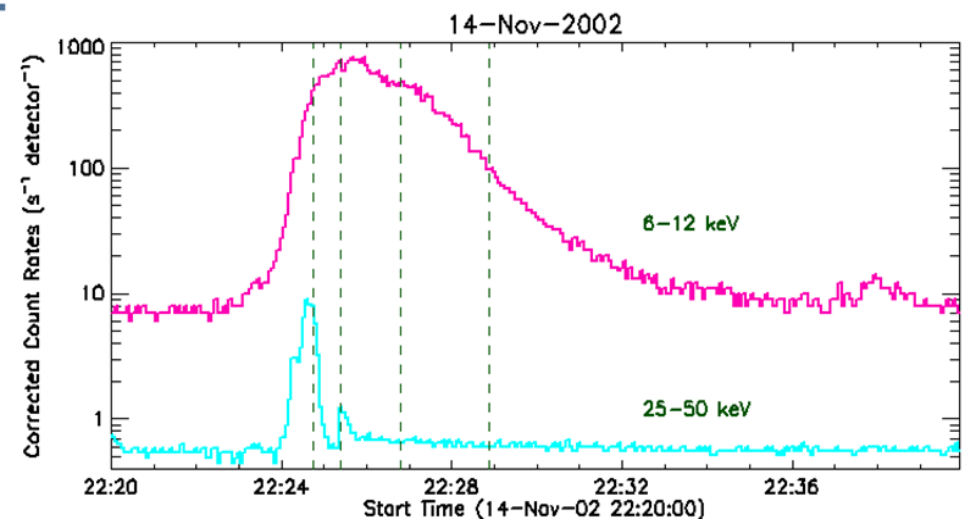

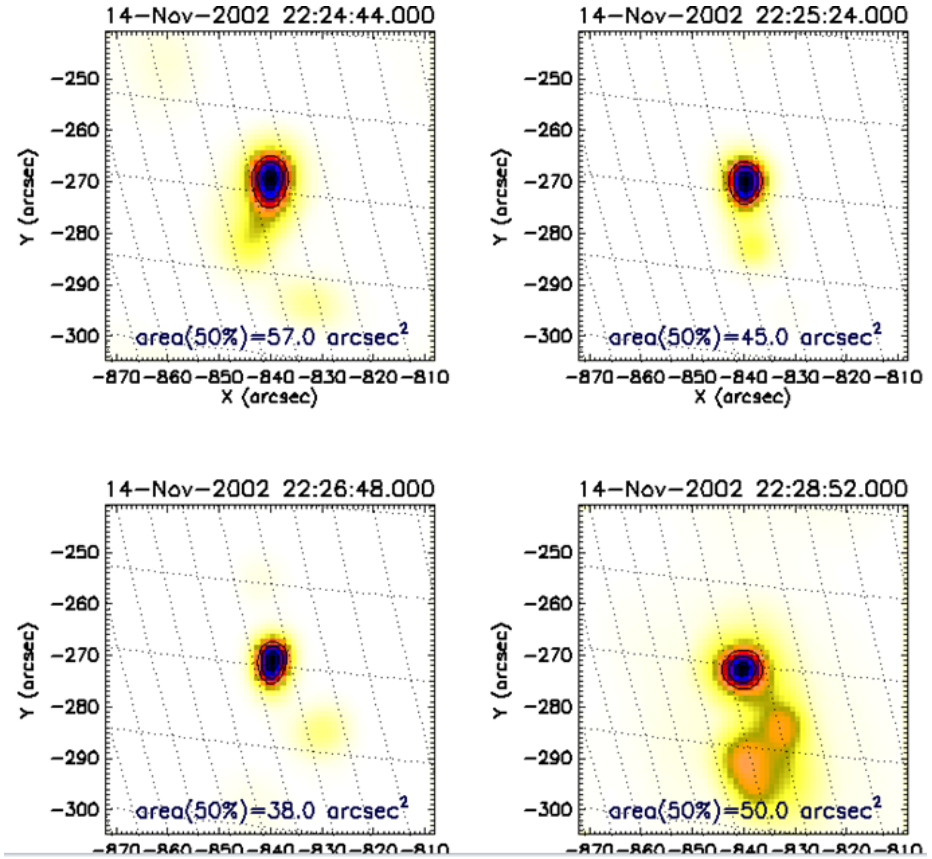

Cooler component is unlikely to significantly contribute to 6-7 keV *RHESSI* emission so we assign the estimated source size with our **hoter** temperature component and determine **the density of hotter plasma from respective EM values**.

Average size (for 50% isophote) obtained based on 49 PIXON reconstructed images covering whole flare evolution is:

3.7 arcsec (5.8 x 10^8 cm)

Flare thermodynamics

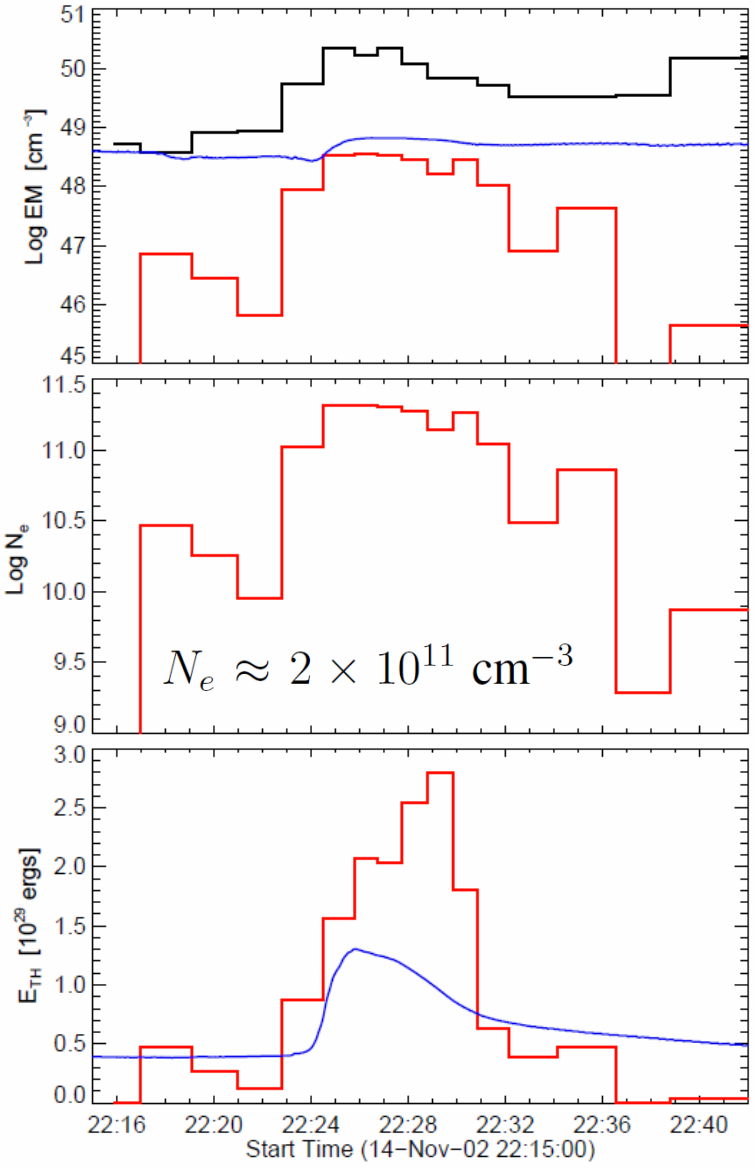

Top: The time evolution of the total emission measure for the cooler (T < 9 MK, **black**) and hotter (T > 9 MK, **red**) plasmas. The **blue** solid line is the emission measure EM_{GOES} as determined from the flux ratio of the *GOES* band fluxes.

Center: Plasma densities derived from the emission measure fluence of the hotter component and source size

***The* thermal energy E_{th},** estimated using the formula:

$$E_{\rm th}\,|_{N_e=\rm const} = 3k_B \frac{\int T\varphi(T)dT}{\sqrt{\int \varphi(T)dT}}\sqrt{V}$$

E_{th} reaches a max. of ~3 x 10^{29} erg, rather typical for a medium-class flare such as the one analysed.

Similar analysis for other flares

C4.8 SOL2002-12-25T05:46

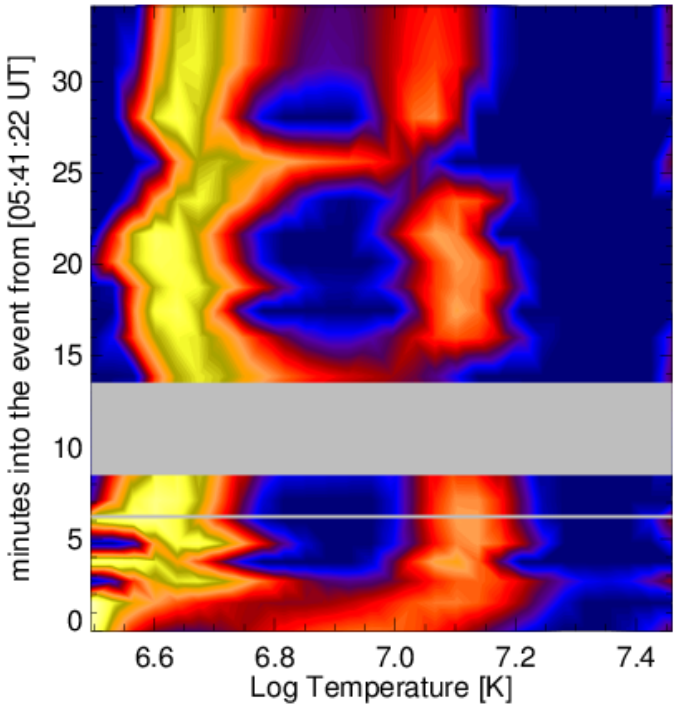

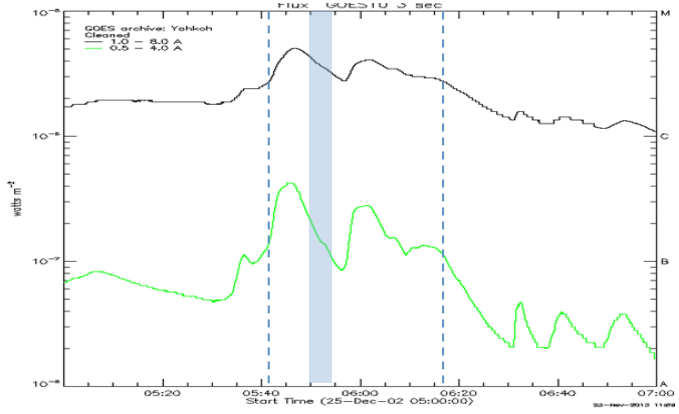

C1.4 SOL2002-12-25T07:34

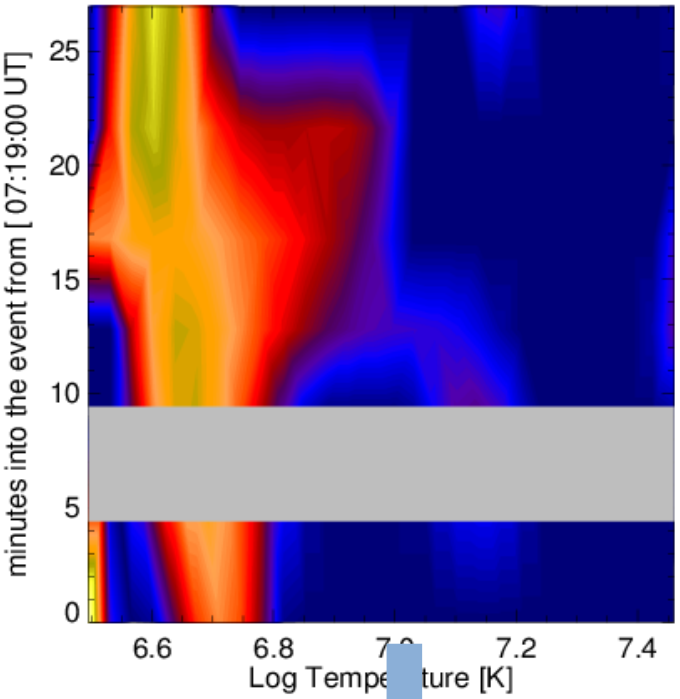

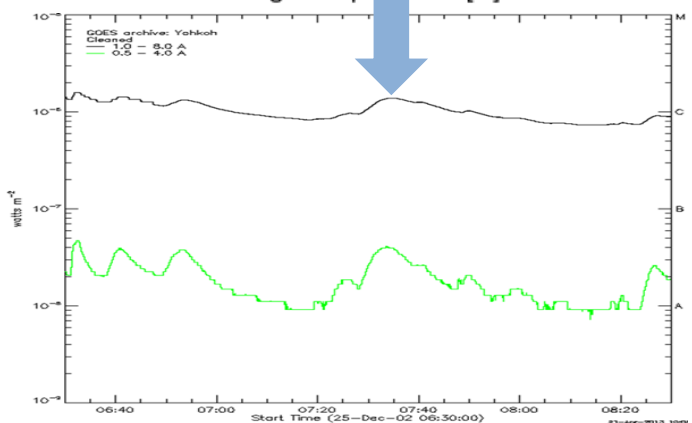

Still other examples

C1.1 SOL2002-12-25T22:48

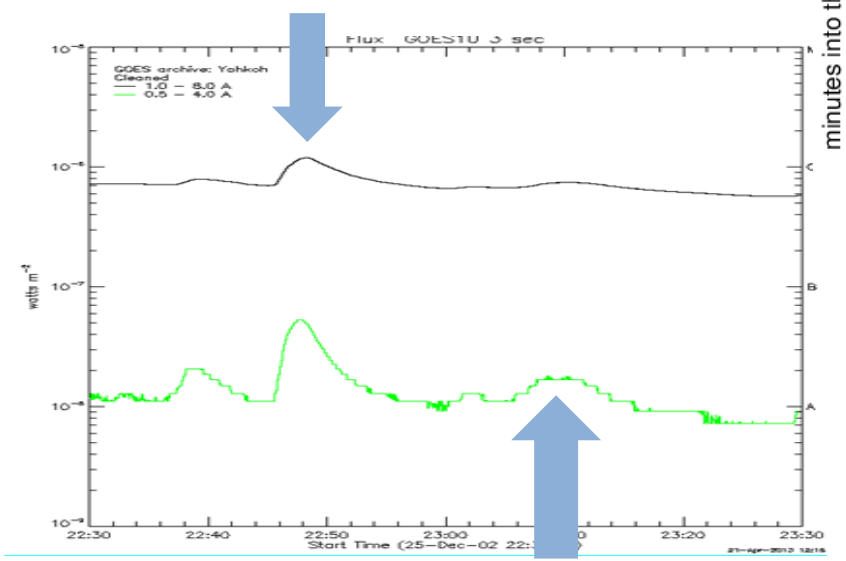

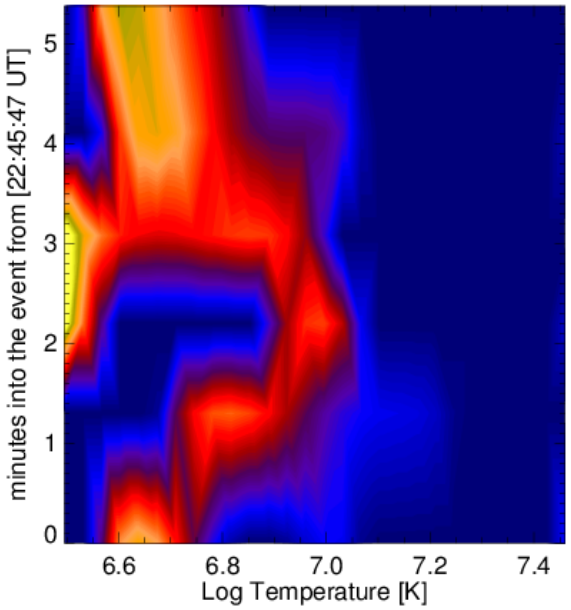

B8.0 SOL2002-12-25T23:10

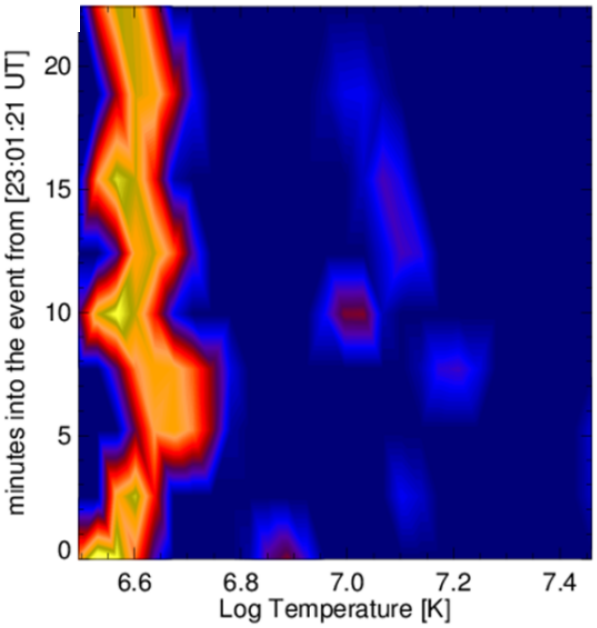

Similar analysis for other flares

C1.9 SOL2002-12-26T08:35

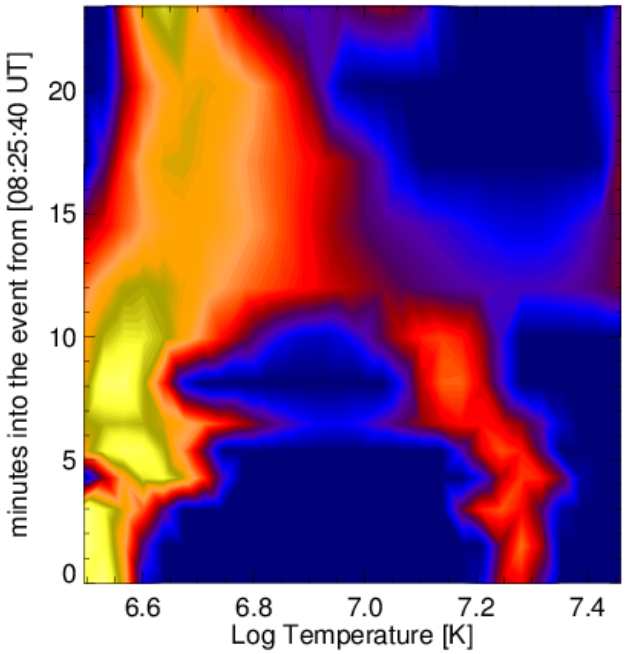

B6.0 SOL2002-12-26T03:52

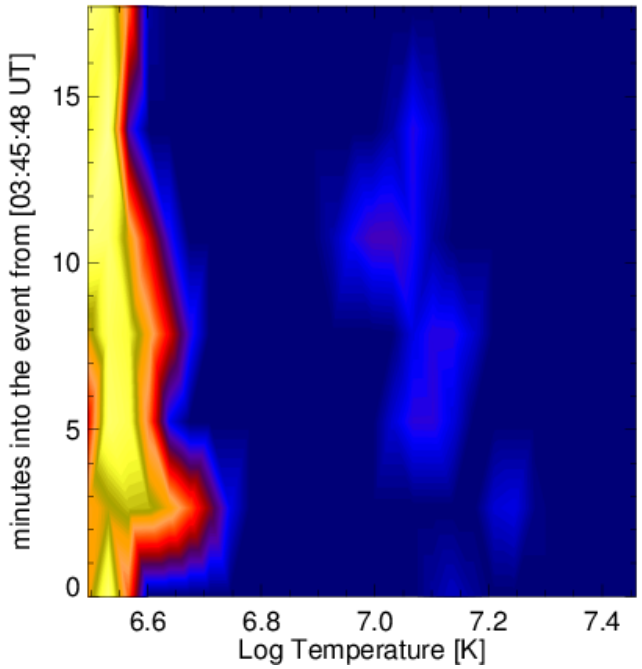

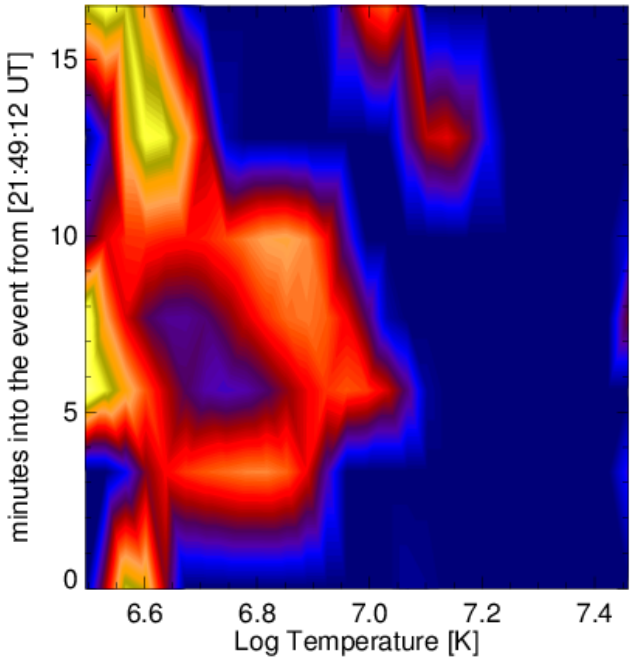

B6.3 SOL2002-12-27T21:58

Take home message

- Plasma composition is **NOT a fixed pattern**- individual coronal structures: flares, AR's etc. may have their individual patterns to be studied in various ways…this also transfers to analyses of EUV spectra
- The DEM models obtained for several analysed flares are usually two-component indicating the tendency of flaring plasma to concentrate in separate temperature regions:

  a coller component (**T < 9 MK**) and the

  hotter one (with **T > 9 MK**).
- Superhot (>25 MK) componens are detected if apprpriate lines/bands are incorporated into the analysis (Hinotori, Caspi) RESIK is missing really hot lines
- The amount of hotter plasma is orders of magnitude lower in comparison with the cooler one (~ two orders during the maximum phase). However presence of this small amount of hot plasma is necessary to accommodate for the observed fluxes in individual spectral bands.
- The extension of the hotter emitting source **(from *RHESSI* images)** determines the (lower limit) of the **density** and **thermal energy** content for the **hotter source**
- High densities (~10^{11} cm^{-3}) of the hotter plasma components are matching other present estimates.

THANK YOU